Title: Pluto's ocean is capped by gas hydrates

Authors: Shunichi Kamata[1*], Francis Nimmo[2], Yasuhito Sekine[3], Kiyoshi Kuramoto[4], Naoki Noguchi[5], Jun Kimura[6], Atsushi Tani[7]

Affiliations:

[1]Creative Research Institution, Hokkaido University, N21, W10, Kita-ku, Sapporo, 001-0021 Japan.

[2]Department of Earth and Planetary Sciences, University of California, Santa Cruz, 1156 High St., Santa Cruz, CA 95064 USA.

[3]Earth-Life Science Institute, Tokyo Institute of Technology, 2-12-1 Ookayama, Meguro-ku, Tokyo, 152-8550 Japan.

[4]Department of Cosmosciences, Hokkaido University, N10, W8, Kita-ku, Sapporo, 060-0810 Japan.

[5]Graduate School of Technology, Industrial and Social Sciences, Tokushima University, 2-1 Minami-Jousanjima-cho, Tokushima, 770-8506 Japan.

[6]Department of Earth and Space Science, Osaka University, 1-1 Machikaneyama-cho, Toyonaka, 560-0043 Japan.

[7]Department of Human Environmental Science, Kobe University, 3-11 Tsurukabuto, Nada-ku, Kobe, 657-8501 Japan.

[*]Correspondence to: Shunichi Kamata, Hokkaido University, kamata@sci.hokudai.ac.jp

Many icy solar system bodies possess subsurface oceans. At Pluto, Sputnik Planitia's location near the equator suggests the presence of a subsurface ocean and a locally thinned ice shell. To maintain an ocean, Pluto needs to retain heat inside. On the other hand, to maintain large variations in ice shell thickness, Pluto's ice shell needs to be cold. Achieving such an interior structure is problematic. Here we show that the presence of a thin layer of clathrate hydrates (gas hydrates) at the base of the ice shell can explain both the long-term survival of the ocean and the maintenance of shell thickness contrasts. Clathrate hydrates act as a thermal insulator, preventing the ocean from complete freezing while keeping the ice shell cold and immobile. The most likely clathrate guest gas is methane either contained in precursor bodies and/or produced by cracking of organic materials in the hot rocky core. Nitrogen molecules initially contained and/or produced later in the core would likely not be trapped as clathrate hydrates, instead supplying the nitrogen-rich surface and atmosphere. The formation of a thin clathrate hydrate layer capping a subsurface ocean may be an important generic mechanism maintaining long-lived subsurface oceans in relatively large but minimally-heated icy satellites and Kuiper Belt Objects.

Liquid water oceans are thought to exist inside icy satellites of gas giants such as Europa and Enceladus and the icy dwarf planet Pluto[1]. Understanding the survival of subsurface oceans is of fundamental importance not only to planetary science but also to astrobiology. One indication of a subsurface ocean on Pluto is Sputnik Planitia, a ~1000-km-wide basin. It is a topographical low and is located near the equator, indicating that it is a positive gravity anomaly. To make this basin a positive gravity anomaly, a subsurface ocean beneath a locally thinned ice shell (by ~90 km) is inferred[2].

The presence of an ocean suggests a “warm” (i.e., not completely frozen) Pluto. However, unlike icy satellites, tides do not play an important role in heating the dwarf planet[3], and radiogenic heating is insufficient to avoid complete freezing unless the ice shell is highly viscous ($>\sim 10^{16}$ Pa s (ref. 4)). Heat may be retained inside Pluto owing to a thick surface thermal insulating layer resulting from high porosity and a high concentration of nitrogen ice[5]. However, if the ice shell is warm, its viscosity should be low[6]. Substantial viscous flow of ice would then occur, eliminating any local thickness contrasts[7]. Consequently, a locally thinned shell suggests a “cold” Pluto ($<\sim 200$ K at the base of the ice shell[2]). One way to reconcile these contradictory requirements is to depress the freezing point of water by contaminating the ocean with anti-freeze molecules, such as ammonia[2]. However, to avoid substantial viscous relaxation of the ice shell, the ammonia concentration needs to be ~30 wt% (Supplementary Fig. 1). Such a high concentration is hard to justify; the ammonia concentration in comets, whose chemical composition should be representative of Kuiper Belt Objects (KBOs) including Pluto[8], are mostly less than 1 % with respect to water[9]. In addition, an ammonia concentration >20 wt% leads to an ocean density <1000 kg/m^3 (Supplementary Fig. 2, ref. 10), which makes it difficult for Sputnik Planitia to be a positive gravity anomaly[11]. Another possibility is that the viscosity of the ice shell is high due to the presence of high-strength material, such as salts[12] or silicate particles[13]. However, in a multiphase system, the weaker phase (i.e., water ice) dominates the flow[12,13]. Consequently, inhibiting substantial viscous relaxation requires the stronger phase (i.e., salts) to be the dominant component. Such an ice shell would have a high density (e.g., ~1.3 g/cm^3 for a mixture of 50% H_2O ice and 50% epsomite). While the density of the ocean might also be high due to the presence of salts in the ocean[11], their concentrations would be largely controlled by the formation of clay minerals and evaporates in the rocky core, keeping the ocean salinity < 4–5 mol/L or < 10 mol% relative to H_2O (ref. 14) and, thus, the ocean density to be < 1.3 g/cm^3. In order for the ice shell to float on the ocean and for Sputnik Planitia to be a positive gravity anomaly, the ice shell has a density much lower than the ocean (at least by ~0.2 g/cm^3 (ref. 11)), and its major constituent needs to be water ice.

Instead, we propose that the ice shell has a thin layer of clathrate hydrates at its base (Fig. 1). Clathrate hydrates, or gas hydrates, are solids in which water molecules create cages trapping gas molecules[15]. Because the formation temperatures of clathrate hydrates are higher than the melting point of pure water ice[15] and the subsurface ocean is sufficiently pressurized by the overlying ice shell, a freezing ocean would form clathrate hydrates rather than water ice if dissolved gas concentrations are sufficiently high[16]. The thermal conductivity of clathrate hydrates is about a factor of 5–10 smaller than that of water ice[17] and the viscosity of clathrate hydrates is about an order of magnitude higher than that of water ice[18]. Because of these physical properties, a cap of clathrate hydrates would act as a highly viscous thermal insulator between a subsurface ocean and an ice shell. The temperature difference across this layer allows the presence of a subsurface ocean with a temperature near the melting point of pure water ice while the overlying ice shell maintains a much lower temperature at the same time. Its high viscosity would also maintain shell thickness contrasts for a long time.

Global thermal evolution of Pluto:

We first evaluate the effect of clathrate hydrates on the thermal evolution of Pluto using the physical properties of methane hydrates[15,17] ($CH_4 \cdot nH_2O$ where $n \sim 6$)

(Methods). In the absence of clathrate hydrates, a subsurface ocean is expected to freeze completely because thermal convection in the ice shell removes heat effectively from the deep interior[4] (Fig. 2a, b). To maintain a thick subsurface ocean, the ice shell needs to be conductive, requiring a reference viscosity about one or two orders of magnitude higher than 10^{14} Pa s, which is a typical value for terrestrial ice sheets[19]. This may not be impossible but would require an extremely large ice grain size (a few cm)[20]. Interestingly, a thicker surface porous layer[5] leads to a shorter ocean lifetime, because such a layer enhances thermal convection in the ice shell beneath (Supplementary Fig. 3).

In contrast, if clathrate hydrates form, a thick subsurface ocean can be maintained for billions of years even if the reference viscosity of water ice is assumed to be 10^{14} Pa s (Fig. 2c). This is because heat from the ocean cannot be removed efficiently through the clathrate hydrate layer. As the clathrate layer thickens the overlying water ice layer cools, leading to a higher viscosity. Thus, thermal convection in the ice shell becomes less vigorous, further reducing the freezing rate of the ocean (Fig. 2d). Consequently, the clathrate hydrate layer remains thin, while reducing the freezing rate of the ocean. If the clathrate hydrate layer grows from the beginning, its current thickness can reach ~30 km (Supplementary Fig. 4a, b). If its formation is delayed, its current thickness would be reduced (Supplementary Fig. 4c, d). Nevertheless, the efficiency of heat removal decreases significantly and the ocean thickness remains approximately constant following the formation of a clathrate hydrate layer.

As the ocean freezes and the ice shell thickens, the radius and surface area of Pluto increase, leading to the formation of normal faults on the surface[4]. Pluto's surface is covered by many such faults[21], and their pattern indeed supports global expansion of

Pluto[22]. A future detailed image analysis estimating the change of Pluto's radius would provide a constraint on the clathrate hydrate layer thickness and the start timing and/or the duration of clathrate hydrate formation, which would inhibit freezing and faulting.

Viscous relaxation of the ice shell:

We next examine the effect of clathrate hydrates on the timescale of viscous relaxation of the ice shell using the physical properties of methane hydrates[15,17,18] (Methods). The origin of the local interior structure beneath Sputnik Planitia (a thin ice shell above a thick ocean) is considered to be associated with the large impact that formed the Sputnik Planitia basin[2,11]. Although the age of this impact is unknown, the eroded rim of the basin suggests that it is likely to be billions of years[23]. Consequently, the timescale of viscous relaxation should be at least one billion years.

If a clathrate hydrate layer does not exist, shell thickness contrasts can be maintained for only a few million years unless an extremely viscous ice shell and/or an extremely cold ocean is assumed (Fig. 3, Supplementary Fig. 5). In contrast, if a clathrate hydrate layer of a few to 10 km in thickness exists at the base of the ice shell, the timescale of ice shell relaxation is increased even by 3 to 4 orders of magnitudes and can exceed one billion years even if we assume typical pure-water properties both for the water ice layer and the ocean (Fig. 3). Such a large increase in the timescale results from the combined effect of a low temperature in the water ice layer and the high viscosity of clathrate hydrates (Supplementary Fig. 6). Thus, under the presence of a thin clathrate hydrate layer, an extremely ammonia- or salt-rich Pluto is no longer necessary to explain a long viscous relaxation timescale for the ice shell.

Implications for geochemical evolution:

Various gas species can form clathrate hydrates, though some species (e.g., CH_4) occupy clathrate hydrates more readily than others (e.g., N_2). This behavior may explain the unique volatile composition observed on Pluto. Comets contain ~1 % of CH_4 and a few % of CO with respect to water[9], and even these low concentrations are sufficient to form a clathrate hydrate layer several tens of km in thickness (Methods, Supplementary Fig. 7). When Pluto formed, volatiles trapped in precursor bodies would have been partitioned between the atmosphere, ice shell, and the subsurface ocean. Gases may also have been initially trapped as clathrate hydrates near the surface[24], which may also have happened at Titan[25]. At an early stage, primordial CH_4 and CO dissolved in the ocean would likely form mixed clathrate hydrates at depth. Although precursor bodies of Pluto may be rich in CO_2 (ref. 9), CO_2 may not be major guest molecules of clathrate hydrates above the ocean because its high density indicates that CO_2-rich hydrates would not float on the ocean unless the ocean is highly salty (Supplementary Table 1). CO_2 clathrate hydrates at the seafloor could have acted as a thermostat to prevent heat transfer from the core to the ocean. Primordial CO_2, however, may have been converted into CH_4 through hydrothermal reactions within early Pluto under the presence of Fe-Ni metals[26]. Because CH_4 and CO predominantly occupy clathrate hydrates, the components that degassed into the surface-atmosphere system would be rich in other species, such as N_2 (refs 8,27,28). Trapping of CO in deep clathrate hydrates and degassing of N_2 may explain the low CO/N_2 on the surface of Pluto[29]. Further constraints on likely incorporation of cometary species, particularly CO, into clathrate hydrates are desirable, either via experiments or a detailed statistical thermodynamic approach[15].

As clathrate hydrate formation continues, concentrations of dissolved gases decrease if gases are not supplied to the ocean, eventually leading to the formation of pure water ice instead of clathrate hydrates at the interface between the ocean and ice shell. Thus, to form clathrate hydrates continuously in the ocean, secondary gases need to be continuously supplied to the ocean in the later stages. One plausible mechanism to supply gases is thermal cracking of organic materials in the rocky core, which would mainly produce CH_4 (refs 30,31). Organic materials are abundant in cometary solids (~45 wt% of dust grains of 67P/Churyumov-Gerasimenko[32]). Thermogenic CH_4 can be produced where temperatures exceed ~150℃ (ref. 33), and such a condition can be achieved in a large portion of Pluto's core for most of its history[8] (Supplementary Fig. 8). A high-temperature origin of CH_4 would leave a trace in its isotopic composition[34]. N_2 can also be produced via pyrolysis of organic matter when temperatures exceed ~350℃ (ref. 35), though CH_4 would be preferentially trapped in clathrate hydrates[27]. Within a hot and porous core, high-temperature water-rock reactions would also occur. These can produce various gas species depending on many factors, including the redox state of the reactions, but the main gas species would be H_2 for chondritic rocks[36]. However, H_2 hydrates do not form unless H_2 is dominant in gases[37]. If organic materials within the rocky core contact with the hydrothermal fluids, a large quantity of C-bearing gas species, such as CH_4, also would be included in the fluids through hydrothermal decomposition[33]. Thus, under the presence of abundant CH_4, H_2 would be degassed to the surface and rapidly lost to the space because of its small mass. In contrast, heavier N_2 becomes a major volatile at Pluto's surface[38,39]. Gas production processes in a hot rocky core are unlikely to occur in small icy bodies. This may be why CH_4 and N_2 are found only on large KBOs such as Pluto and Eris but not on small KBOs such as

Charon[38,40]. Furthermore, icy bodies possessing subsurface oceans may have low CO/N_2 and/or CH_4/N_2 ratios on their surface.

The current presence of subsurface oceans in outer solar system bodies is often explained by a high concentration of ammonia[1,41], though it is only rarely detected[9,38,42]. In contrast, a thin clathrate hydrate layer is equally effective at maintaining subsurface oceans and preventing motion of the ice shell, while requiring much lower concentrations of secondary species (e.g., CH_4) whose presence is commonly inferred. Such layers provide a likely explanation for minimally-heated but ocean-bearing worlds.

References:

1. Nimmo, F. & Pappalardo, R. T. Ocean worlds in the outer solar system. *J. Geophys. Res.* **121**, 1378–1399 (2016)
2. Nimmo, F. et al. Reorientation of Sputnik Planitia implies a subsurface ocean on Pluto. *Nature* **540**, 94–96 (2016)
3. Hussmann, H., Sotin, C. & Lunine, J. I. Interiors and evolution of icy satellites. In *Treatise in Geophysics* 2nd edn (eds. Schubert, G.) Vol. 10 *Physics of Terrestrial Planets and Moons*, 605–635 (Elsevier, 2015)
4. Robuchon, G. & Nimmo, F. Thermal evolution of Pluto and implications for surface tectonics and a subsurface ocean. *Icarus* **216**, 426–439 (2011)
5. Hammond, N. P., Barr, A. C. & Parmentier, E. M. Recent tectonic activity on Pluto driven by phase changes in the ice shell. *Geophys. Res. Lett.* **43**, 6775–6782 (2016)
6. Durham, W. B., Prieto-Ballesteros, O., Goldsby, D. L. & Kargel, J. S. Rheological

and thermal properties of icy materials. *Space Sci. Rev.* **153**, 273–298 (2010)

7. Kamata, S. & Nimmo, F. Interior thermal state of Enceladus inferred from the viscoelastic state of the ice shell. *Icarus* **284**, 387–393 (2017)
8. McKinnon, W. B., Simonelli, D. P. & Schubert, G. Composition, internal structure, and thermal evolution of Pluto and Charon. In *Pluto and Charon* (eds. Stern, S. A. & Tholen, D. J.) 295–346 (Univ. Arizona Press, 1997).
9. Le Roy, L. et al. Inventory of the volatiles on comet 67P/Churyumov-Gerasimenko from Rosetta/ROSINA. *Astron. Astrophys.* **583**, A1 (2015)
10. Croft, S. K., Lunine, J. I. & Kargel, J. Equation of state of ammonia–water liquid: Derivation and planetological applications. *Icarus* **73**, 279–293 (1988)
11. Johnson, B. C., Bowling, T. J., Trowbridge, A. J. & Freed, A. M. Formation of the Sputnik Planum basin and the thickness of Pluto's subsurface ocean. *Geophys. Res. Lett.* **43**, 10068–10077 (2016)
12. Durham, W. B., Stern, L. A., Kubo, T. & Kirby, S. H. Flow strength of highly hydrated Mg- and Na-sulfate hydrate salts, pure and in mixtures with water ice, with application to Europa. *J. Geophys. Res.* **110**, E12010 (2005)
13. Durham, W. B., Kirby, S. H. & Stern, L. A. Effects of dispersed particulates on the rheology of water ice at planetary conditions. *J. Geophys. Res.* **97**, 20883–20897 (1992)
14. Zolotov, M. Y. Aqueous fluid composition in CI chondritic materials: Chemical equilibrium assessments in closed systems. *Icarus* **220**, 713–729 (2012)
15. Sloan, E. D. & Koh, C. A. *Clathrate hydrates of natural gases* 3^{rd} edn. (CRC Press, 2007)
16. Choukroun, M., Kieffer, S. W., Lu, X. & Tobie, G. Clathrate hydrates: Implications

for exchange processes in the outer Solar System. In *The Science of Solar System Ices* (eds. Gudipati, M. S. & Castillo-Rogez, J.) 409–454 (Splinger-Verlag NY, 2013)

17. Waite, W. F., Stern, L. A., Kirby, S. H., Winters, W. J. & Mason, D. H. Simultaneous determination of thermal conductivity, thermal diffusivity and specific heat in sI methane hydrate. *Geophys. J. Int.* **169**, 767–774 (2007)
18. Durham, W. B., Kirby, S. H., Stern, L. A. & Zhang, W. The strength and rheology of methane clathrate hydrate. *J. Geophys. Res.* **108**, 2182 (2003)
19. Tobie, G., Choblet, G. & Sotin, C. Tidally heated convection: Constraints on Europa's ice shell thickness. *J. Geophys. Res.* **108**, 5124 (2003)
20. Barr, A. C. & McKinnon, W. B. Convection in ice I shells and mantles with self-consistent grain size. *J. Geophys. Res.* **112**, E02012 (2007)
21. Moore, J. M. et al. The geology of Pluto and Charon through the eyes of New Horizons. *Science* **351**, 1284–1293 (2016)
22. Keane, J. T., Matsuyama, I., Kamata, S. & Steckloff, J. K. Reorientation and faulting of Pluto due to volatile loading within Sputnik Planitia. *Nature* **540**, 90–93 (2016)
23. White, O. L. et al. Geological mapping of Sputnik Planitia on Pluto. *Icarus* **287**, 261–286 (2017)
24. Mousis, O. et al. Methane clathrates in the Solar System. *Astrobiology* **15**, 308–326 (2015)
25. Lunine, J. I. & Stevenson, D. J. Thermodynamics of clathrate hydrate at low and high pressures with application to the outer Solar System. *Astrophys. J. Suppl.* **58**, 493–531 (1985)

26. McCollom, T. M. & Seewald, J. S. Experimental constraints on the hydrothermal activity of organic acids and acid anions: I. Formic acid and formate. *Geochim. Cosmochim. Acta* **67**, 19, 3625–3644 (2003).

27. Herri, J.-M. et al. Gas hydrate equilibria for CO_2–N_2 and CO_2–CH_4 gas mixtures—Experimental studies and thermodynamic modelling. *Fluid Phase Equilib.* **301**, 171–190 (2011)

28. Patt, A., Simon, J.-M., Picaud, S. & Salazar, J. M. A Grand Canonical Monte Carlo study of the N_2, CO, and mixed N_2–CO clathrate hydrates. *J. Phys. Chem. C* **122**, 18432–18444 (2018)

29. Glein, C. R. & Waite, J. H. Primordial N_2 provides a cosmochemical explanation for the existence of Sputnik Planitia, Pluto. *Icarus* **313**, 79–92 (2018)

30. Claypool, G. E. & Kvenvolden, K. A. Methane and other hydrocarbon gases in marine sediment. *Ann. Rev. Earth Planet. Sci.* **11**, 299–327 (1983)

31. McKinnon, W. B. & Mueller, S. Pluto's structure and composition suggest origin in the solar, not a planetary, nebula. *Nature* **335**, 240–243 (1988)

32. Bardyn, A. et al. Carbon-rich dust in comet 67P/Churyumov-Gerasimenko measured by COSIMA/Rosetta. *Mon. Not. R. Astron. Soc.* **469**, S712–S722 (2017)

33. Seewald, J. S. Organic–inorganic interactions in petroleum-producing sedimentary basins. *Nature* **426**, 327–333 (2003)

34. Stopler, D. A. et al. Formation temperatures of thermogenic and biogenic methane. *Science* **344**, 1500–1503 (2014)

35. Behar, F., Gillaizeau, B., Derenne, S., Largeau, C. Nitrogen distribution in the pyrolysis products of a type II kerogen (Cenomanian, Italy). Timing of molecular nitrogen production versus other gases. *Energy Fuels* **14**, 431–440 (2000)

36. Sekine, Y. et al. High-temperature water-rock interactions and hydrothermal environments in the chondrite-like core of Enceladus. *Nat. Commun.* **6**, 8604 (2015)

37. Skiba, S. S., Larionov, E. G., Manakov, A. Y., Kolesov, B. A. & Kosyakov, V. I. Investigation of hydrate formation in the system H_2−CH_4−H_2O at a pressure up to 250 MPa. *J. Phys. Chem. B* **111**, 11214–11220 (2007)

38. Grundy, W. M. et al. Surface compositions across Pluto and Charon. *Science* **351**, aad9189 (2016)

39. Gladstone, G. R. et al. The atmosphere of Pluto as observed by New Horizons. *Science* **351**, aad8866 (2016)

40. Barucci, M. A., Brown, M. E., Emery, J. P. & Merlin, F. Composition and surface properties of transneptunian objects and Centaurs. In *The Solar System beyond Neptune* (eds. Barucci, M. A. Boehnhardt, H., Cruikshank, D. P. & Morbidelli, A.) 143–160 (Univ. Arizona Press, 2008).

41. Hussmann, H., Sohl, F. & Spohn, T. Subsurface oceans and deep interiors of medium-sized outer planet satellites and large trans-neptunian objects. *Icarus* **185**, 258–273 (2006)

42. Waite, J. H. et al. Liquid water on Enceladus from observations of ammonia and ^{40}Ar in the plume. *Nature* **460**, 487–490 (2009)

Acknowledgments: This study was supported by KAKENHI from the Japan Society for Promotion of Science (Grant Nos. JP16K17787, JP17H06456, and JP17H06457).

Author contributions: S.K. developed the idea of this study, conducted thermal evolution and viscous relaxation calculations, created all figures, and was the primary author of the manuscript. F.N. participated in numerous discussions and co-wrote the manuscript. Y.S. and K.K. provided information on gas production mechanisms and likely guest gas species of clathrate hydrates. N.N. provided detailed information on clathrate hydrates and calculated their densities. J.K. participated in numerous discussions on thermal evolution models. A.T. provided detailed information on clathrate hydrates formation. All the authors participated in interpretation of the results.

Author Information: The authors declare no competing financial interests. Correspondence and requests for materials should be addressed to S.K. (kamata@sci.hokudai.ac.jp).

Figures:

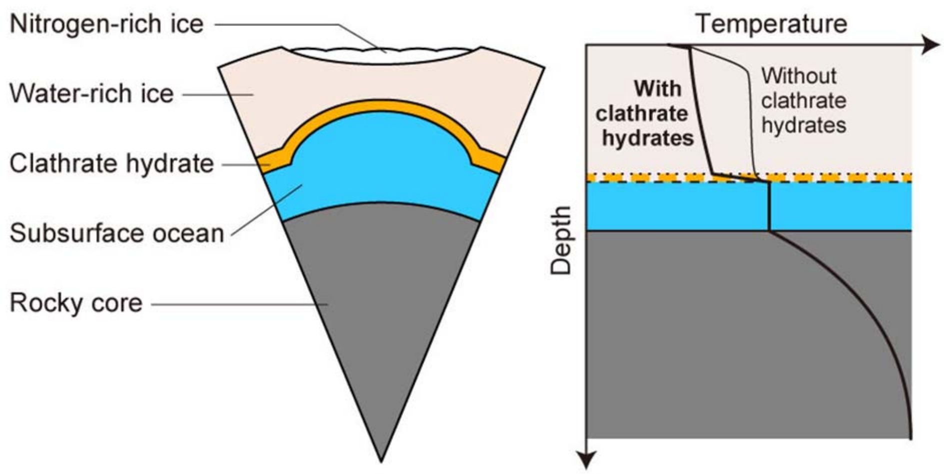

Figure 1 | Schematic diagram of the interior structure of Pluto. The ice shell has a thin clathrate hydrate layer at its base. Temperature changes substantially across this layer immediately above the subsurface ocean, leading to a conductive shell rather than a convective shell. Nitrogen-rich ice on the surface is the bright surface of Sputnik Planitia.

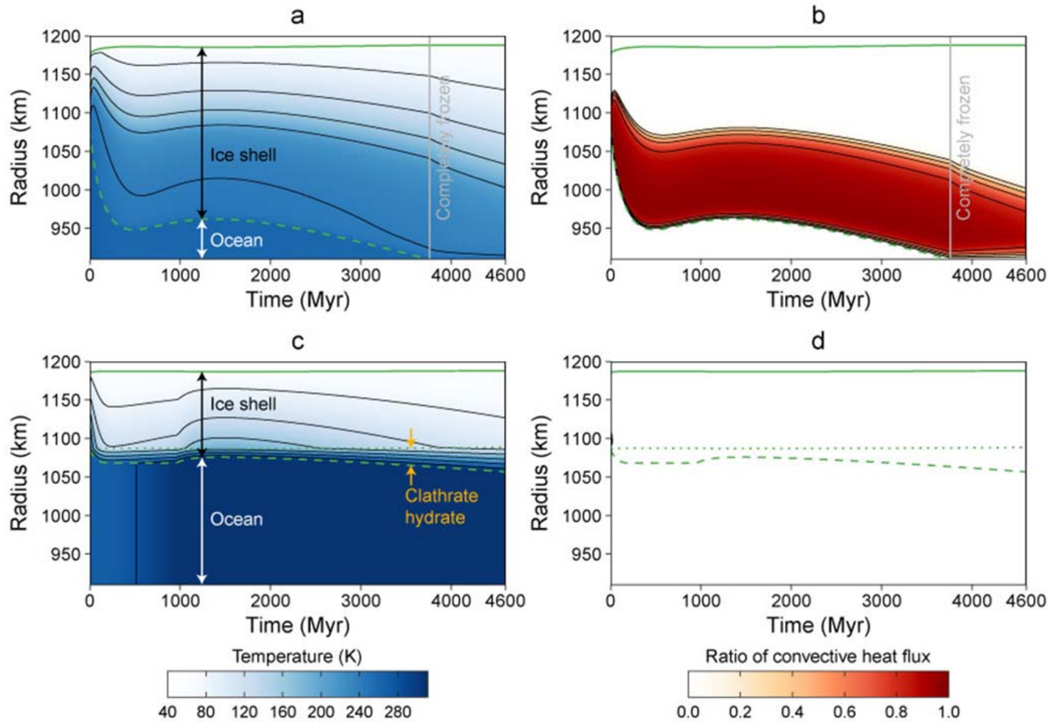

Figure 2 | Time evolution of the interior thermal profile above the rocky core. Here the reference viscosity of water ice is 10^{14} Pa s, the initial ice shell thickness is 100 km, and the surface insulating layer thickness is 5 km. The green solid, dashed, and dotted curves indicate the surface of Pluto, the boundary between the ice shell and the ocean, and the boundary between the water ice layer and the clathrate hydrate layer, respectively. **a**, The temperature profile for the case without clathrate hydrate formation. The subsurface ocean becomes thin rapidly and freezes completely at ~3.8 Gyr. **b**, The ratio of the convective heat flux to the total heat flux (the sum of the convective and conductive heat fluxes) for the case of **a**. The lower part of the ice shell where temperature is nearly constant is highly convective. **c**, The temperature profile for the case with clathrate hydrate formation. Clathrate hydrate formation starts from the beginning (0 yr). The subsurface ocean remains thick, and the water ice layer is cold throughout. **d**, The ratio of the convective heat flux to the total heat flux for the case of **c**. Convection does not occur in the ice shell.

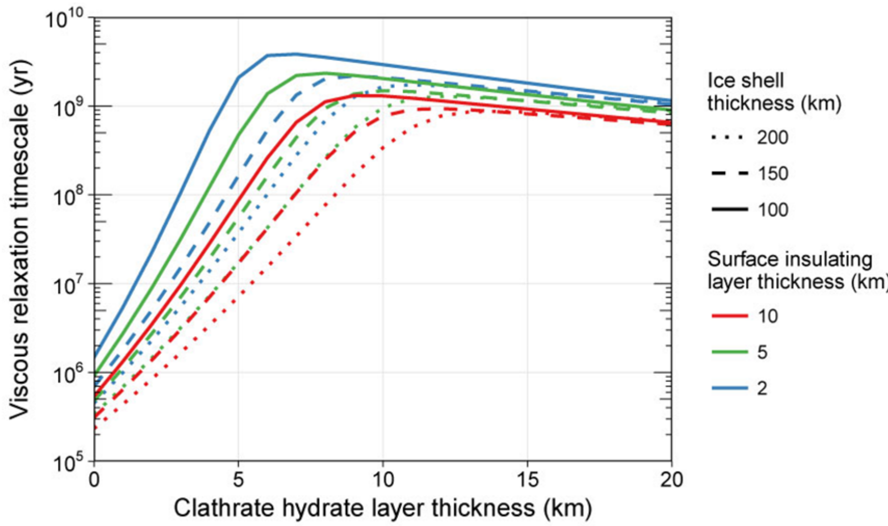

Figure 3 | Timescale of viscous relaxation of the ice shell. Results for different layer thicknesses are shown. The reference viscosity of water ice is 10^{14} Pa s, and freezing-point depression due to impurities in the ocean is not considered. The presence of a clathrate hydrate layer ~5–10 km in thickness leads to a timescale of viscous relaxation longer than 10^9 yr.

Methods:

Thermal evolution:

To calculate the time evolution of the radial temperature profile of Pluto, we used the code developed by ref. 43. We modified the code to incorporate the effects of a clathrate layer and those of a surface thermal insulating layer.

We assume a 3-layer Pluto, consisting of an ice shell (solid), a subsurface ocean (liquid), and a rocky core (solid). The time evolution of temperature in the solid parts is obtained by solving the equation:

$$\rho C_p \frac{dT}{dt} = -\frac{1}{r^2}\frac{d}{dr}(r^2 F_{\mathrm{cond}} + r^2 F_{\mathrm{conv}}) + Q \qquad (1)$$

where ρ is density, C_p is specific heat, T is temperature, t is time, r is radial distance from the center, F_{cond} is conductive heat flux, F_{conv} is convective heat flux, and Q is volumetric heating rate. F_{cond} is given by the product of thermal conductivity and the local thermal gradient while F_{conv} is estimated using a modified mixing length theory[43] (see below).

The core is assumed to be purely conductive (F_{conv} = 0 W/m^2) and to be uniformly heated from within due to the decay of long-lived radioactive elements. The heating rate for carbonaceous chondrites[4,43] is used. The density, specific heat, and thermal conductivity of the core are 3000 kg/m^3, 1000 J/kg/K, and 3 W/m/K, respectively. The radius of the core is ≈910 km, which is calculated from eq. (2) of ref. 5 assuming the mean density of Pluto[44] (1854 kg/m^3), the present-day radius of Pluto[44] (1188 km), and the density of ices (including clathrate hydrates; 920 kg/m^3).

The subsurface ocean is assumed to be an inviscid fluid, and the ocean temperature is assumed to be uniform. For the case without clathrate hydrate formation, the ocean temperature is calculated from the pressure-dependent melting point of pure water ice[45]. For the case with clathrate hydrate formation, it is between the melting point of pure water ice and the dissociation temperature of methane hydrate[15]. No heat production in the ocean is assumed.

The ice shell is divided into 3 layers: a surface insulating layer (i.e., a top low-conductivity layer), a water ice layer, and a basal clathrate hydrate layer. The thickness of the top layer is assumed to be constant and to be 5 km unless otherwise noted. The thin top and basal layers are assumed to be purely conductive, and the thick intermediate layer is assumed to be convective or conductive depending on the viscosity. The thermal conductivities from the top to the bottom layers are 1 W/m/K (ref. 5), 0.4685 + 488.49/T W/m/K where T is temperature in Kelvin (ref. 46), and 0.6 W/m/K (ref. 17), respectively. The temperature-dependent specific heat of water ice[47] and that of methane hydrate[48] are used. No heat production (Q = 0 W/m^3) in the ice shell is assumed. F_{conv} for the intermediate part is given by

$$F_{\mathrm{conv}} = \begin{cases} -\frac{\alpha C_p \rho^2 g l}{18\eta}\left\{\frac{dT}{dr} - \left(\frac{dT}{dr}\right)_s\right\} \ (\text{for } \frac{dT}{dr} \le \left(\frac{dT}{dr}\right)_s) \\ 0 \ \ (\text{for } \frac{dT}{dr} > \left(\frac{dT}{dr}\right)_s) \end{cases} \quad (2)$$

where $\alpha = 10^{-4}$ /K is thermal expansivity of ice, g is gravitational acceleration, l is the mixing length, η is viscosity of ice, and $(dT/dr)_s$ is the adiabatic thermal gradient. dT/dr is calculated by local thermal gradient, while $(dT/dr)_s$ is given by $-\alpha g T/C_p$. l is chosen so that it reproduces a scaling law between the Rayleigh number and the Nusselt number based on 3D numerical calculations[43,49]. l is updated at each time step since it depends on the thickness of the layer, rheological parameters, and the temperature difference across the layer[43]. η is given by

$$\eta = \eta_{\mathrm{ref}} \exp\left(\frac{E_a}{R_g T_{\mathrm{ref}}}\left(\frac{T_{\mathrm{ref}}}{T} - 1\right)\right) \quad (3)$$

where η_{ref} is reference viscosity of ice, E_a = 60 kJ/mol is the activation energy, R_g is the gas constant, T_{ref} = 273 K is the reference temperature[4,43,50]. The nominal value of η_{ref} is 10^{14} Pa s (ref. 19). Note that we assume a Newtonian rheology. This assumption is appropriate under typical conditions for terrestrial ice sheets (i.e., grain size ~ 1 mm, stress ~ 10^{-3} MPa, temperature near the melting point) (ref. 51). Nevertheless, Pluto's ice shell may exhibit non-Newtonian behavior (due to a large grain size, for example). The effect of non-Newtonian flow can be imitated by a Newtonian fluid with a smaller activation energy[52,53]. Calculation results using different activation energies are shown in Supplementary Fig. 9. We find that a smaller activation energy leads to a faster freezing of a subsurface ocean beneath a convective ice shell. Consequently, our model calculations using a Newtonian rheology provide the longest ocean lifetime for cases without a clathrate hydrate layer. On the hand, for cases with a clathrate hydrate layer, different activation energies lead to nearly the same result because the ice shell is conductive. Thus, our conclusion does not change even if Pluto's ice shell exhibits non-Newtonian behavior. It is noted that results shown in Supplementary Fig. 9 assume the reference viscosity of water ice of 10^{14} Pa s. Although different creep mechanisms may lead to different reference viscosities, its quantification is left for another study.

The initial thickness of the ice shell is assumed to be 100 km. Initial temperature in the ice shell linearly increases with depth from 40 K at the surface to the pressure-dependent melting point of water ice[45] at the base of the ice shell. The initial temperature of the ocean and the rocky core is assumed to be uniform (i.e., the melting point of water ice). Different initial conditions do not affect the long-term evolution[4,43]. The exception is an initially completely frozen case; ref. 4 reported that a subsurface ocean does not appear if an initially completely frozen Pluto and $\eta_{ref} \leq 10^{15}$ Pa s are assumed. However, the conditions required for the formation of a subsurface ocean based on their results are too strict because a freezing-point depression due to pressure is not incorporated in their calculations. A detailed investigation of such conditions is beyond the scope of this study and is left for another study.

The temporal change in the thickness of the ice shell is calculated from the difference between the outgoing and incoming heat fluxes at the base of the ice shell. Note that this difference in heat flux is used not only to change the thickness of the ice shell but also to change the temperature of the ocean. For the case without clathrate hydrate formation, the effect of the ocean temperature change caused by a change in the ice shell thickness is incorporated by using an effective latent heat[43]. For the cases with clathrate hydrate formation, the change in the thickness of the ice shell is interpreted as that of the clathrate hydrate layer. If the outgoing heat flux is higher than the incoming heat flux, the clathrate hydrate layer becomes thicker, keeping the ocean temperature constant. If the outgoing heat flux is lower than the incoming heat flux, the ocean temperature increases, keeping the layer constant until the ocean temperature reaches the pressure-dependent dissociation temperature of methane hydrate[15]. If the ocean temperature reaches the dissociation temperature, the clathrate hydrate layer becomes thinner. As the clathrate hydrate layer becomes thinner and the pressure at the top of the ocean decreases, the ocean temperature decreases because of the pressure dependence of dissociation temperature. Similar to the case without clathrate hydrate formation, the effect of pressure dependence of dissociation temperature is included by using an effective latent heat. Latent heats of water ice and methane hydrate are 333 kJ/kg and 437 kJ/kg (ref. 54), respectively. Note that the radius of Pluto changes as the thicknesses of the ice shell and the ocean (the density of 1000 kg/m^3 is assumed for the latter) change in order to conserve the total mass of Pluto. The initial radius of Pluto is determined so that the final radius becomes the present-day value through trial and error.

The surface temperature is fixed to 40 K, and the thermal gradient at the center is fixed to 0 K/m. The temperatures at the base of the ice shell and the top of the rocky core are the same and are given by temperature of the ocean if a subsurface ocean exists. If the ocean is completely solidified, the temperature at the boundary between the ice shell and the rocky core is obtained by equating the heat flux at the top of the rocky core to that at the base of the ice shell. Temperatures and heat fluxes at the boundaries within the ice shell are assumed to be continuous. For the case with clathrate hydrate formation, the start time of clathrate hydrate formation of 0 yr and no pre-existing clathrate hydrate layer are assumed unless otherwise noted. We calculate the thermal evolution for 4.6 Gyr for each calculation.

Viscous relaxation:

To calculate the timescale of viscous relaxation for the ice shell of Pluto, we followed the procedure adopted by ref. 7. We assume that the thinned portion of the ice shell has a bowl-shaped topography at the base of the ice shell. More specifically, the cross section can be described using a quadratic function, and the height and radius of the bowl are assumed to be 80 km and 500 km, respectively. These values are chosen assuming a nearly (Airy) isostatically compensated basin before the loading of nitrogen-rich ice[2,11]. The shape of the basal topography is then expressed as a superposition of zonal components of spherical harmonic functions. In this study, we consider spherical harmonic degrees from 1 to 20. The time evolution of the amplitudes (coefficients) of each spherical harmonic for 10^{10} yr is obtained using the numerical code calculating spheroidal viscoelastic deformation of a planetary body developed by ref. 55 (see below). The time evolution of the basal topography can be calculated by superposing the spherical harmonics with time-dependent amplitudes. The timescale of viscous relaxation is defined as the time when the volume of the bowl becomes $1/e$ of the initial condition where e is Napier's constant.

The governing equations are the linearized equation of momentum conservation given by

$$\nabla_j \cdot \left(\sigma_{ij} - P\delta_{ji}\right) + \rho \nabla_i \phi = 0, \tag{4}$$

the Poisson's equation for the gravitational field given by

$$\nabla^2 \phi = -4\pi G \rho, \tag{5}$$

and the constitutive equation for a Maxwell medium given by

$$\frac{d\sigma_{ji}}{dt} + \frac{\mu}{\eta}\left(\sigma_{ji} - \frac{\sigma_{kk}}{3}\delta_{ji}\right) = \left(\kappa - \frac{2\mu}{3}\right)\frac{de_{kk}}{dt}\delta_{ji} + 2\mu\frac{de_{ji}}{dt}, \tag{6}$$

where ∇_i is a spatial differentiation in direction of i (= x, y, z), σ_{ji} is stress tensor, e_{ji} is strain tensor, P is hydrostatic pressure, δ is the Kronecker delta, ϕ is gravitational potential, G is the gravitational constant, ρ is density, μ is shear modulus, η is viscosity, κ is bulk modulus. Application of spectral harmonic expansion to the governing equations leads to a six-component, time-dependent, inhomogeneous first-order ordinary differential equation system. The major assumptions are a spherically-symmetric steady-state interior structure, small deformation amplitudes, and a linear viscoelasticity[55]. These assumptions are valid to estimate the timescale of viscous relaxation, though more detailed numerical calculations would be necessary for precisely estimating the shape of the ice shell.

Following the thermal evolution calculations, we use a 3-layer Pluto model, though a steady-state thermal profile is adopted because what we calculate is the timescale of viscous relaxation under a given interior structure. We assume that the ice shell consists of Maxwell viscoelastic material, that the subsurface ocean is an inviscid liquid, and that the rocky core consists of purely elastic material. The radius of the core is determined in the same manner as that done in thermal evolution calculations. Different ice shell thicknesses, clathrate hydrate layer thicknesses, and surface insulating layer thicknesses are considered.

The densities of the ice shell, the ocean, and the core are 920 kg/m^3, 1000 kg/m^3, and 3000 kg/m^3, respectively, which are used in the thermal evolution calculations. The shear moduli of the ice shell, the ocean, and the core are 3.3 GPa, 0 GPa, and 10 GPa, respectively. We adopt an incompressible ($\kappa \rightarrow \infty$ and $e_{kk} \rightarrow 0$) limit because of the small size of Pluto. The viscosity in the ice shell is calculated from the temperature profile adopting the same rheological model. The surface temperature is fixed to 40 K. The temperature at the base of the ice shell is assumed to be the pressure-dependent melting point of pure water ice[56] unless otherwise noted. Assuming a steady-state conductive profile with given boundary temperatures, we calculate the temperature profile in the ice shell analytically. The thermal conductivity profile is the same as that used in thermal evolution calculations. The reference viscosities of water ice and clathrate hydrates are 10^{14} Pa s (ref. 19) and 2×10^{15} Pa s (ref. 18), respectively, unless otherwise noted. The activation energy of water ice and clathrate hydrates are 60 kJ/mol (ref. 50) and 90 kJ/mol (ref. 18), respectively, unless otherwise noted. The upper limit of the viscosity is 10^{30} Pa s, though the choice of this value does not affect the timescale of viscous relaxation of topography at the base of the ice shell.

Mass balance:

We calculate the amount of methane with respect to water in the ice shell and subsurface ocean. The thicknesses of these layers are determined in the same manner as in viscous relaxation calculations; the thickness of the ice shell is a free parameter while that of the ocean is calculated so that the mean density becomes the observed value. The ice shell is divided into an outer pure water ice layer and a deeper methane hydrate layer. We assume methane hydrate (Structure I) of full cage occupancy (i.e., $CH_4 \cdot 5.75\ H_2O$) (ref. 15). The ocean is assumed to consist of water and methane only. We use the pressure at the top of the ocean and the melting point of pure water ice[56] to calculate the (pressure- and temperature-dependent) solubility of methane in the ocean[57].

Data availability:

The data that support the plots within this paper and other findings of this study are available from the corresponding author on reasonable request.

Code availability:

Codes for the thermal evolution and viscous relaxation calculations are available upon reasonable request from S.K.

References (Methods):

43. Kamata, S. One-dimensional convective thermal evolution calculation using a modified mixing length theory: Application to Saturnian icy satellites. *J. Geophys.*

Res. **123**, 93–112 (2018)

44. Nimmo, F. et al. Mean radius and shape of Pluto and Charon from New Horizons images. *Icarus* **287**, 12–29 (2017)
45. Leliwa-Kopystyński, J., Maruyama, M. & Nakajima, T. The water–ammonia phase diagram up to 300 MPa: Application to icy satellites. *Icarus* **159**, 518–528 (2002)
46. Hobbs, P. V. *Ice physics* (Oxford University Press, 1974)
47. Choukroun, M. & Grasset, O. Thermodynamic data and modeling of the water and ammonia-water phase diagrams up to 2.2 GPa for planetary geophysics. *J. Chem. Phys.* **133**, 144502 (2010)
48. Circone, S., Kirby, S. H. & Stern, L. A. Thermodynamic calculations in the system CH_4-H_2O and methane hydrate phase equilibria. *J. Phys. Chem. B.* **110**, 8232–8239 (2006)
49. Yao, C., Deschamps, F., Lowman, J. P., Sanchez-Valle, C. & Tackley, P. J. Stagnant lid convection in bottom-heated thin 3-D spherical shells: Influence of curvature and implications for dwarf planets and icy moons. *J. Geophys. Res.* **119**, 1895–1913 (2014)
50. Goldsby, D. L. & Kohlstedt, D. L. Superplastic deformation of ice: Experimental observations. *J. Geophys. Res.* **106**, 11017–11030 (2001)
51. Barr, A. C. & Pappalardo, R. T. Onset of convection in the icy Galilean satellites: Influence of rheology. *J. Geophys. Res.* **110**, E12005 (2005)
52. Christensen, U. R. Convection in a variable-viscosity fluid: Newtonian versus power-law rheology. *Earth Planet. Sci. Lett.* **64**, 153–162 (1983)
53. Dumoulin, C., Doin, M.-P. & Fleitout, L. Heat transport in stagnant lid convection with temperature- and pressure-dependent Newtonian or non-Newtonian rheology.

J. Geophys. Res. **104**, 12759–12777 (1999)

54. Anderson, G. K. Enthalpy of dissociation and hydration number of methane hydrate from the Clapeyron equation. *J. Chem. Thermodyn.* **36**, 1119–1127 (2004)
55. Kamata, S., Sugita, S. & Abe, Y. A new spectral calculation scheme for long-term deformation of Maxwellian planetary bodies. *J. Geophys. Res.* **117**, E02004 (2012)
56. Choukroun, M. & Grasset, O. Thermodynamic model for water and high-pressure ices up to 2.2 GPa and down to the metastable domain. *J. Chem. Phys.* **127**, 124506 (2007)
57. Duan, Z. & Mao, S. A thermodynamic model for calculating methane solubility, density and gas phase composition of methane-bearing aqueous fluids from 273 to 523 K and from 1 to 2000 bar. *Geochim. Cosmochim. Acta* **70**, 3369–3386 (2006)

Supplementary Information: Pluto's ocean is capped by gas hydrates

Shunichi Kamata, Francis Nimmo, Yasuhito Sekine, Kiyoshi Kuramoto, Naoki Noguchi, Jun Kimura, Atsushi Tani

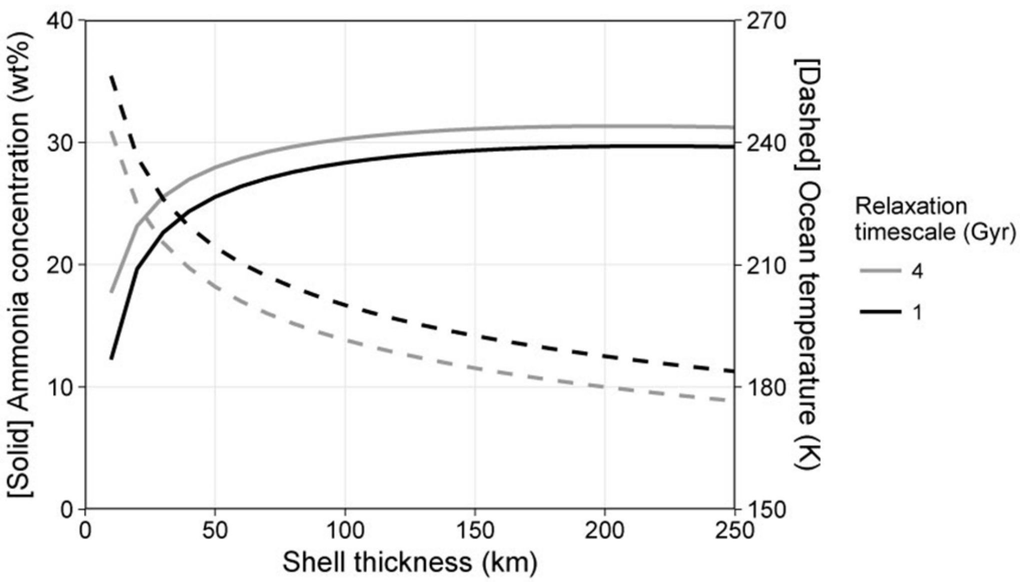

Supplementary Fig. 1 | Ammonia concentration and temperature of the subsurface ocean required for avoiding substantial lateral flow in the ice shell without clathrate hydrates. The ocean temperature is calculated analytically by using the method of ref. 2. The corresponding ammonia concentration is calculated from an equation based on laboratory experiments[45]. A shell thickness less than ~100 km is unlikely because the height of the thickened portion of the ocean is expected to be ~80 km for an isostatically compensated basin 7 km in depth[2,11] before the loading of nitrogen ice sheet.

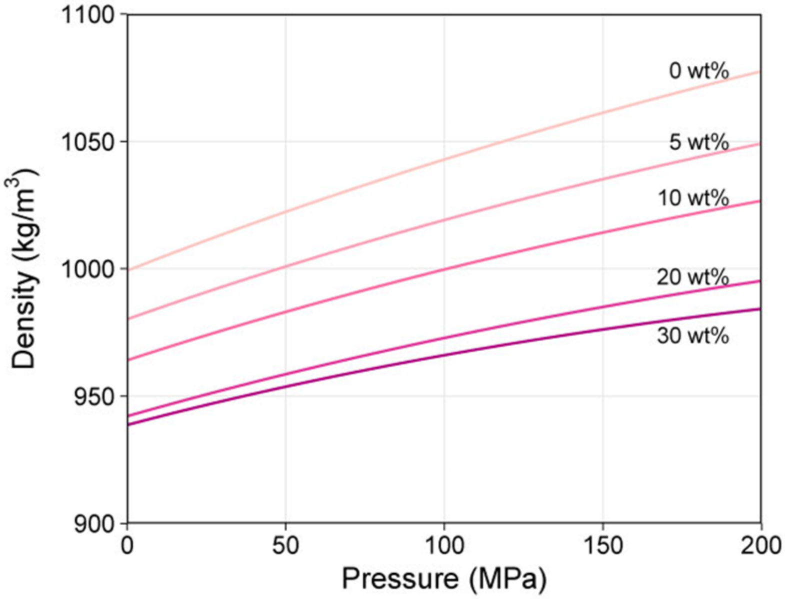

Supplementary Fig. 2 | Density of ammonia-water liquid. The density is calculated analytically by using the method of ref. 10. The temperature is assumed to be the melting point depending on pressure and ammonia concentration[45]. An ammonia concentration ≥20 wt% is unlikely because the ocean density becomes <1000 kg/m^3, which will make the Sputnik Planitia basin a negative gravity anomaly[11].

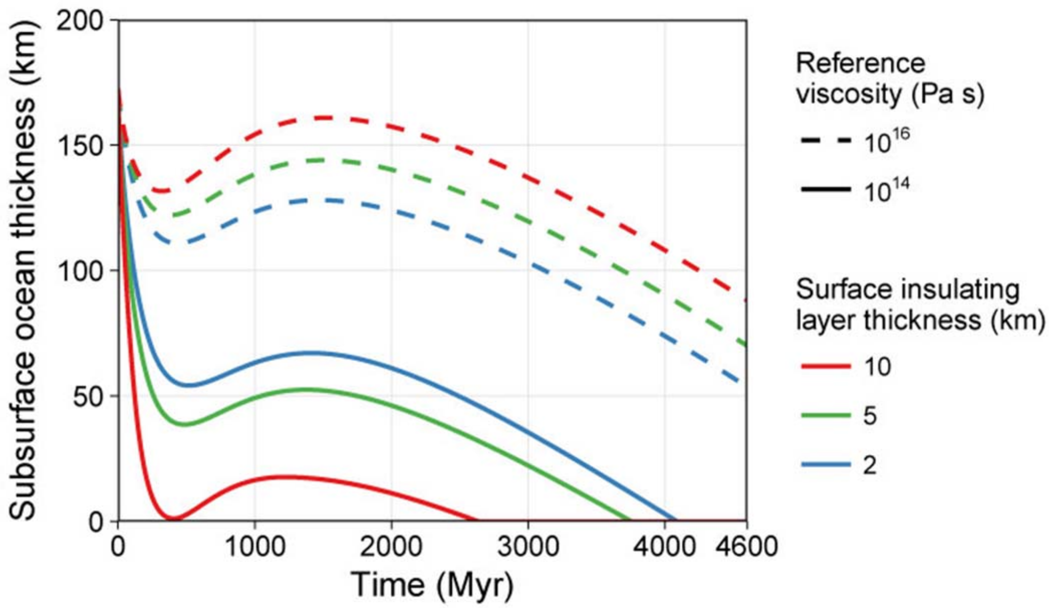

Supplementary Fig. 3 | Time evolution of the subsurface ocean thickness for cases without clathrate hydrates. Results for different reference viscosities of water ice and different thicknesses of a surface insulating layer are shown. A high reference viscosity results in a conductive ice shell. In such a case, a thicker surface insulating layer leads to a thicker ocean. In contrast, a low reference viscosity results in a convective ice shell, and the effect of a surface insulating layer becomes opposite from the case of a conductive shell (see text).

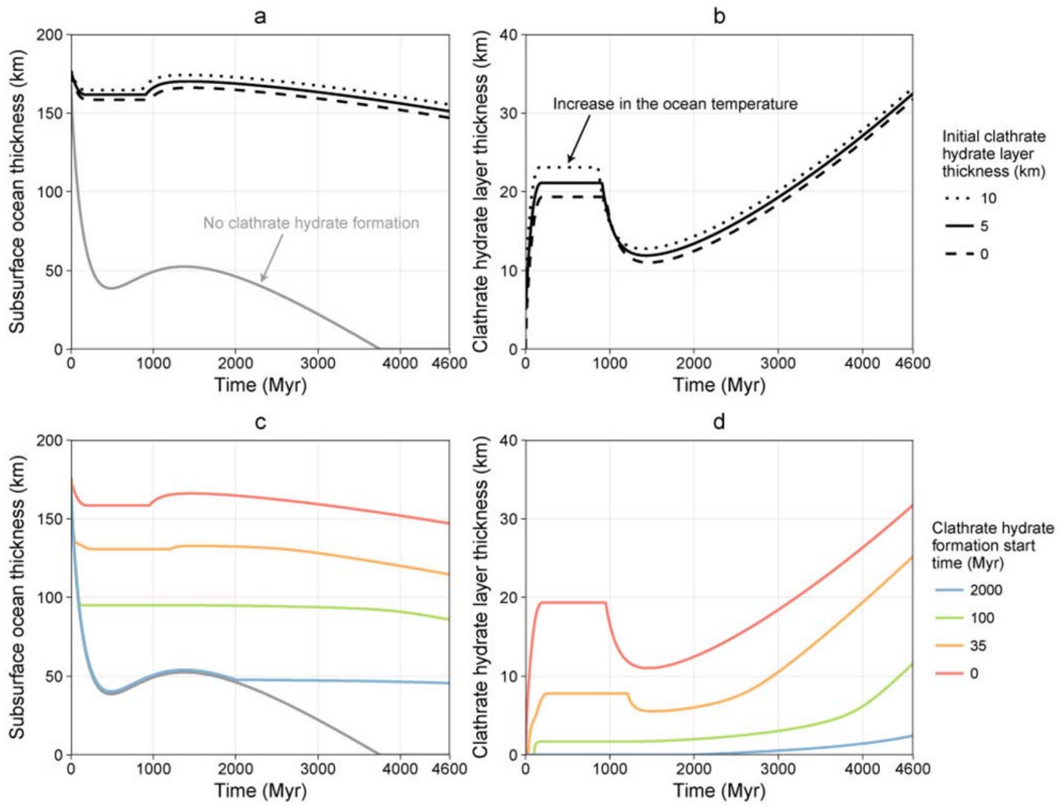

Supplementary Fig. 4 | Time evolution of Pluto's interior structure for cases with and without clathrate hydrate layers. Here the reference viscosity of water ice is 10^{14} Pa s, the initial ice shell thickness is 100 km, and the surface insulating layer thickness is 5 km. **a**, The evolution of the subsurface ocean thickness for different pre-existing clathrate hydrate layer thicknesses. Clathrate hydrate formation starts from the beginning (0 yr). The gray line represents the result without clathrate hydrates. **b**, The evolution of clathrate hydrate layer thickness for the results shown in **a**. The thickness of the clathrate hydrate layer reaches ~30 km. **c**, The same as **a** but for different start timings of the clathrate hydrate formation. No pre-existing clathrate hydrate layer is assumed. **d**, The same as **b** but for the results shown in **c**. An earlier start of clathrate hydrates formation leads to a thicker clathrate hydrate layer.

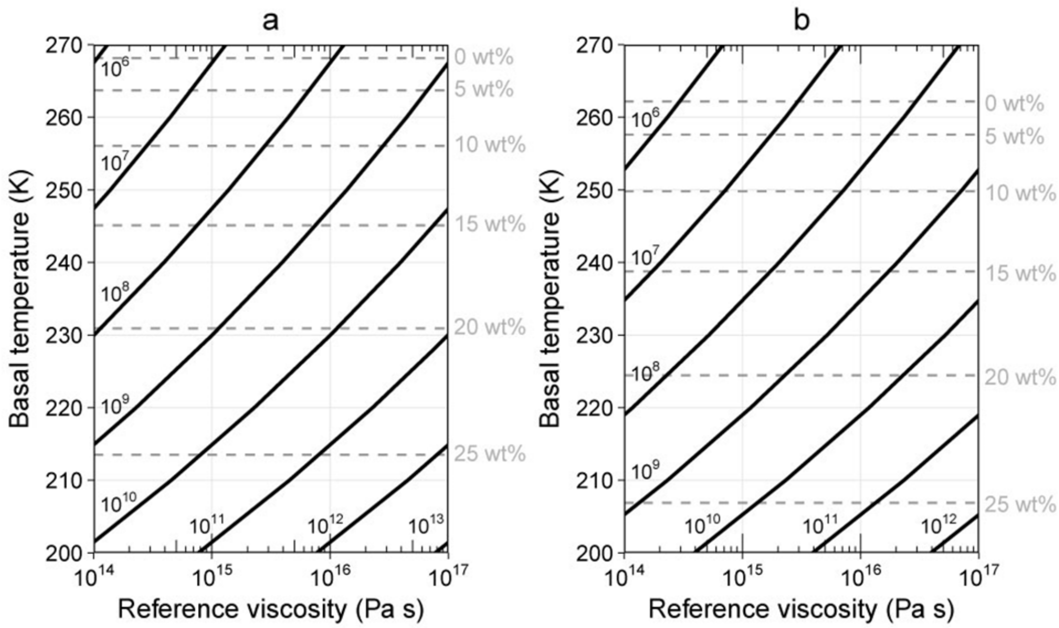

Supplementary Fig. 5 | Timescale of viscous relaxation of the ice shell without clathrate hydrates. Results for the ice shell thickness of **a** 100 km and of **b** 200 km, respectively, are shown. The surface insulating layer thickness is 5 km. Numbers indicate the relaxation timescale in yr. Horizontal gray lines show corresponding ammonia contents in the ocean[45]. The nominal model (i.e., a reference viscosity of 10^{14} Pa s and an ammonia concentration of 0 wt%) leads to a relaxation timescale of only ~10^6 yr.

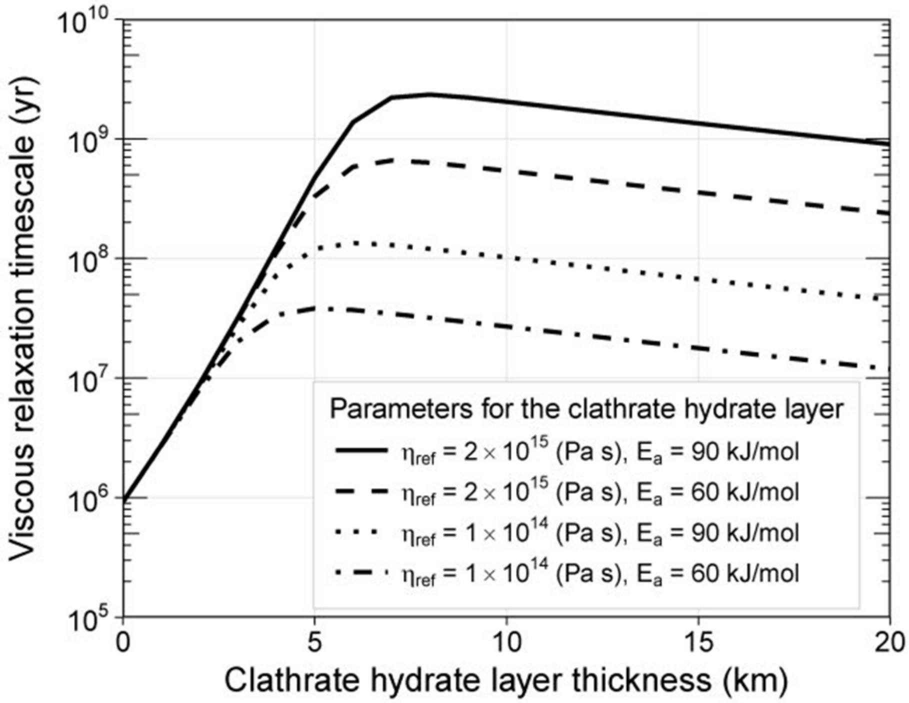

Supplementary Fig. 6 | Timescale of viscous relaxation of the ice shell assuming different rheological parameters for the clathrate hydrate layer. Here the reference viscosity of water ice is 10^{14} Pa s, the ice shell thickness is 100 km, the surface insulating layer thickness is 5 km, and freezing-point depression due to impurities in the ocean is not considered. The presence of a clathrate hydrate layer ~5 km in thickness increases the relaxation timescale by a factor of ~30. Both a reference viscosity and an activation energy of clathrate hydrates higher than those of pure water ice increase the relaxation timescale.

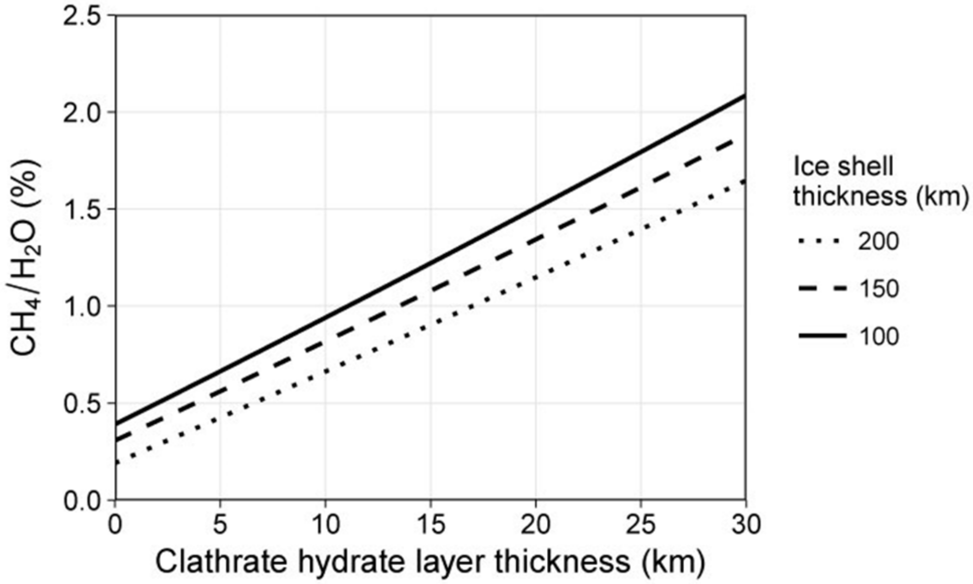

Supplementary Fig. 7 | The amount of methane with respect to water required to form a methane hydrate layer. Results for different ice shell thicknesses are shown. Methane hydrate (Structure I) of full cage occupancy is assumed (i.e., $CH_4 \cdot 5.75\ H_2O$). A thinner ice shell requires a larger amount of methane because of a thicker subsurface ocean that can dissolve methane. One percent of methane is sufficient to form a clathrate hydrate layer >10 km in thickness.

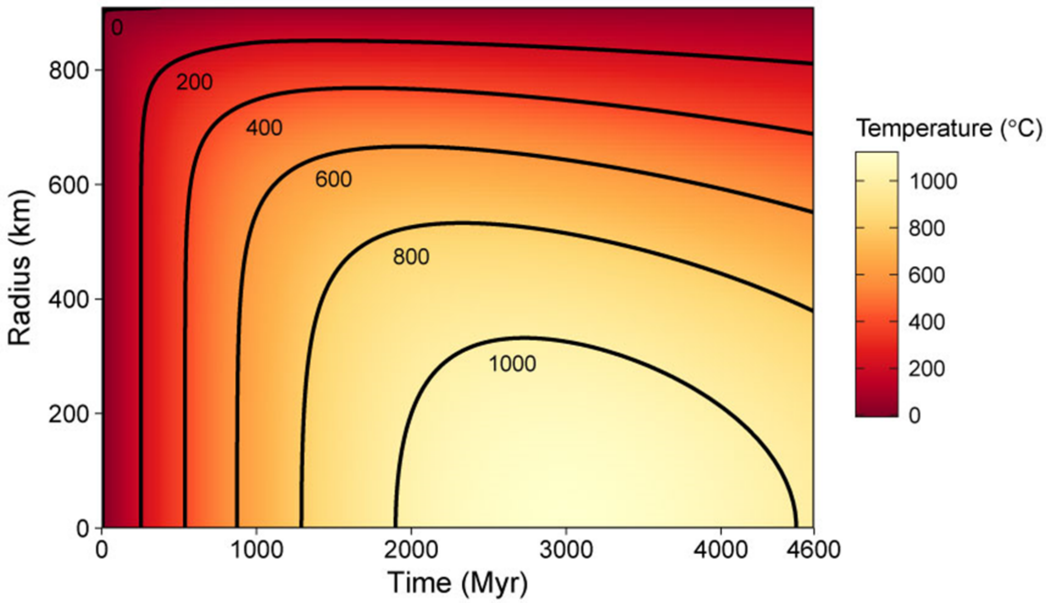

Supplementary Fig. 8 | Time evolution of temperature in the rocky core. The result for the nominal case with clathrate hydrate formation (i.e., the lower panels in Fig. 2) is shown. Different calculation conditions lead to similar temperature profiles in the core. A large portion of the core has temperature higher than ~150℃ (CH_4 production) and ~350℃ (N_2 production) for billions of years[8].

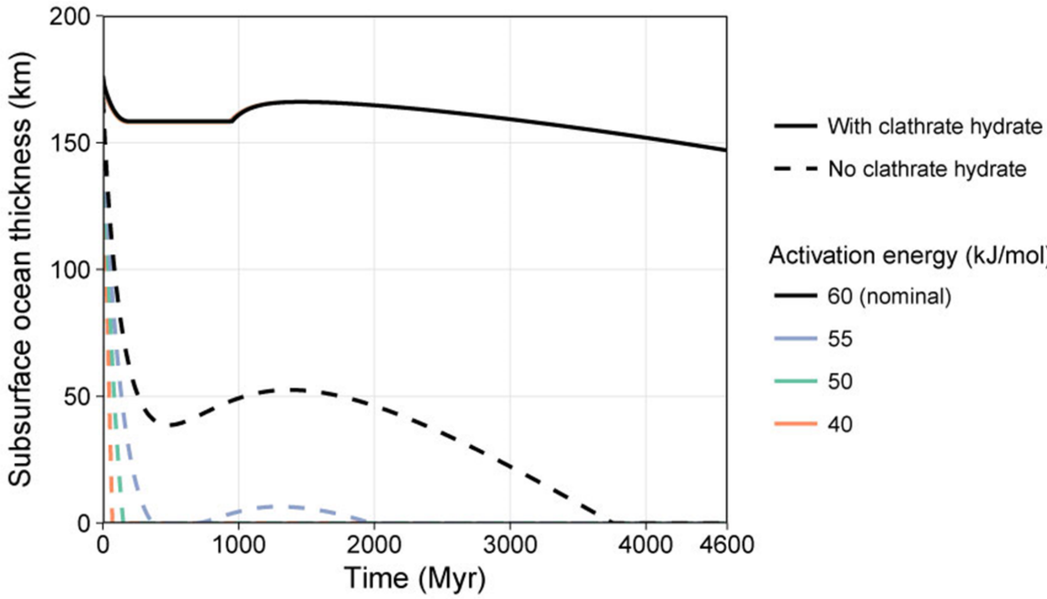

Supplementary Fig. 9 | Time evolution of the subsurface ocean thickness for different activation energies. Results for cases with and without clathrate hydrates under a given reference viscosity (i.e., 10^{14} Pa s) are shown. The use of a smaller activation energy can approximately reproduce the thermal structure assuming a non-Newtonian rheology[52,53]. If a clathrate hydrate layer does not exist, a smaller activation energy leads to a faster freezing of a subsurface ocean. In contrast, if a clathrate hydrate layer exists, different activation energies leads to nearly the same result because the ice shell is conductive (see Fig. 2).

Supplementary Table 1 | Density of clathrate hydrates.

Guest molecules	Structure	Density (kg/m^3)
CH_4	Structure I	918.55
CO	Structure I	1010.8
CO	Structure II	1000.5
CO_2	Structure I	1133.8
N_2	Structure II	1000.5

Each density is calculated by the method of ref. 15. The cage occupancies of the guest molecules are assumed to be 1.0.